HHS Public Access

Author manuscript

J Vasc Res. Author manuscript; available in PMC 2023 July 07.

Published in final edited form as:

J Vasc Res. 2022 ; 59(5): 261–274. doi:10.1159/000525258.

Smooth muscle cell Notch2 is not required for atherosclerotic plaque formation in ApoE null mice

Jessica Davis-Knowlton[a,b], **Jacqueline E. Turner**[a], **Anne Harrington**[a], **Lucy Liaw**[a,b]

[a]Center for Molecular Medicine, Maine Medical Center Research Institute, MaineHealth, Scarborough, ME, USA

[b]Tufts Graduate School of Biomedical Sciences, Boston, MA, USA

Abstract

Introduction.—We previously identified Notch2 in smooth muscle cells (SMC) in human atherosclerosis, and found that signaling via Notch2 suppressed human SMC proliferation. Thus, we te-sted whether loss of Notch2 in SMC would alter atherosclerotic plaque progression using a mouse model.

Methods.—Atherogenesis was examined at the brachiocephalic artery and aortic root in a vascular SMC null (inducible smooth muscle-myosin heavy chain Cre) Notch2 strain on the $ApoE^{-/-}$ background. We measured plaque morphology and size, as well as lipid, inflammation and smooth muscle actin content after western diet.

Results.—We generated an inducible SMC Notch2 null on the $ApoE^{-/-}$ background. We observed ~90% recombination efficiency with no detectable Notch2 in SMC. Loss of SMC Notch2 did not significantly change plaque size, lipid content, necrotic core, or medial area. However, loss of SMC Notch2 reduced contractile SMC in brachiocephalic artery lesions and increased inflammatory content in aortic root lesions after 6 weeks of western diet. These changes were not present with loss of SMC Notch2 after 14 weeks of western diet.

Conclusions.—Our data show that loss of SMC Notch2 does not significantly reduce atherosclerotic lesion formation, although in early stages of plaque formation there are changes in SMC and inflammation.

Corresponding Author: Lucy Liaw PhD, Center for Molecular Medicine, Maine Medical Center Research Institute, MaineHealth, 81 Research Drive, Scarborough, ME 04074 USA, Tel: 207-396-8142, Lucy.Liaw@mainehealth.org.

Author Contributions

Jessica Davis-Knowlton and Lucy Liaw contributed to conception and design of the study, and Jessica Davis-Knowlton completed the majority of the experimental work and data analysis. Jacqueline Turner performed histological and immunostaining and some morphometric tracing. Anne Harrington developed breeding strategies, had oversight of mouse husbandry and genotyping, and performed AAV inoculation. Jessica Davis-Knowlton wrote the first draft of the manuscript. All authors contributed to manuscript revision, read, and approved the submitted version. Lucy Liaw provided funding, resources, and oversight of the project.

Statement of Ethics

This study protocol was reviewed and approved by the Institutional Animal Care and Use Committee of Maine Medical Center, protocol 2110 (Liaw PI).

Data Availability Statement

The data that support the findings of this study are openly available in Figshare at https://doi.org/10.6084/m9.figshare.16671115.v2, reference number 16671115.v2

Conflict of Interest Statement

The authors have no conflicts of interest to declare.

Keywords

atherosclerosis; Notch; smooth muscle cell; phenotype switching; apolipoprotein E

Introduction

Notch is an important signaling molecule in vascular development and repair and regulates atherosclerosis in a tissue and receptor/ligand dependent manner. Proinflammatory cytokine treatment of endothelial cells suppressed Notch1 expression and hemizygous deletion of Notch1 in endothelial cells increased predisposition to atherosclerosis [1,2]. The delta-like ligand 4 (Dll4)/Notch1 axis promoted the M1 proinflammatory phenotype in macrophages [3,4], and inhibition of signaling using neutralizing anti-Dll4 antibodies reduced accumulation of macrophages, decreased fat mass, and attenuated insulin resistance [5]. Notch regulation of vascular SMC phenotype and function is also important in vascular SMC proliferative diseases [6,7]. The effects of Notch signaling in adult vascular SMC are complex and receptor dependent, and while many cells are present in complex plaques, lineage tracing studies have shown that SMC represent up to 70% of cells representing a wide spectrum of phenotypes [8–11].

Vascular SMC expressed Notch1 promotes proliferation and cell survival, Notch2 promotes contractile differentiation and inhibits proliferation, and Notch3 promotes both contractile differentiation and proliferation [7]. We previously showed that Jagged1 activation of Notch2 mediated a unique suppression of proliferation in human vascular SMC [12]. Jagged1 activation of Notch2 in atherosclerotic vascular SMC derived from endarterectomy samples also suppressed proliferation but failed to induce smooth muscle actin expression as it does in healthy vascular SMC [13]. SMC deletion of Notch effector, CBF1/RBPjκ/Su(H)/Lag1, prevented cap SMC from re-acquiring contractile smooth muscle actin expression, while overexpression of Notch intracellular domain to produce forced Notch signaling inhibited medial SMC contribution to plaques [14]. However, these previous studies did not specifically address the Notch protein responsible for these effects. Based on our previous data that Notch2 suppresses human vascular SMC proliferation, we hypothesized that Notch2 may be an endogenous inhibitor of atherogenesis via suppression of SMC growth. Thus, we engineered loss of Notch2 from vascular SMC in a mouse model of atherosclerosis. Our findings indicate that suppression of Notch2 in SMC does not significantly change the overall progression of atherosclerosis in the mouse.

Materials and Methods

Mouse Models.

Studies were approved by the Institutional Animal Care and Use Committee of Maine Medical Center. All mice were on the C57BL/6 background. Athero-susceptible mice with inducible smooth muscle myosin heavy chain (SMMHC)-specific Notch2 deletion were generated by crossing *Notch2*$^{flox/flox}$ [15]× SMMHC-CreER^{T2} mice [16,17] (Jackson Laboratory, #01052, #019079) with *ApoE*$^{-/-}$ mice [18] (Jackson Laboratory #002052). In *Notch2*$^{flox/flox}$ mice, loxP sites flank exon 3 of *Notch2* [15]. *ApoE*$^{-/-}$ × *Notch2*$^{flox/flox}$

× SMMHC-CreER$^{T2Cre/0}$ mice were randomized to receive either 1mg tamoxifen i.p. in 100μL corn oil or vehicle control daily for 5d at 5–7 weeks of age. The *ApoE*$^{-/-}$ × *Notch2*$^{flox/flox}$ × SMMHC-CreER$^{T2Cre/0}$ mice are referred to as ApoE$^{-/-}$;N2$^{SMC\text{-}null}$, and corn-oil treated *ApoE*$^{-/-}$ × *Notch2*$^{flox/flox}$ × SMMHC-CreER$^{T2Cre/0}$ littermates are referred to as ApoE$^{-/-}$;N2$^{SMC\text{-}ctr}$.

Genotyping.

Genomic DNA was isolated by alkaline lysis. PCR was performed using 5PRIME MasterMix for the *ApoE* allele at a 68°C annealing temperature using the primers (5'-GCCTAGCCGAGGGAGAGCCG-3'), (5'-TGTGACTTGGGAGCTCTGCAGC-3'), and (5'-GCCGCCCCGACTGCATCT-3'). This resulted in a 155 bp band from the wildtype and a 245bp product from the mutant allele. PCR to amplify the *Notch2* allele was performed at an annealing temperature of 60°C. *Notch2*$^{fl/fl}$ primers (5'-TAGGAAGCAGCTCAGCTCACAG-3', 5'-ATAACGCTAAACGTGCACTGGAG-3') yielded a 161bp band from the wildtype and a 20bp product from the floxed allele. The SMMHCCreER^{T2} genotyping was performed at an annealing temperature of 58°C using primers (5'-TCCAACCTGCTGACTGTG-3', 5'-TCAGAGTTCTCCATCAGGG-3'), yielding a 455bp transgenic product.

Induction of atherosclerosis and tissue collection.

ApoE$^{-/-}$;N2$^{SMC\text{-}ctr}$ and ApoE$^{-/-}$;N2$^{SMC\text{-}null}$ littermates were fed western diet (Research Diets D12079B, 41% calories from fat) for 6 weeks, or fed western diet (Envigo Teklad TD.88137, 42% calories from fat) for 14 weeks. Feeding started 7d after the last injection of tamoxifen/vehicle. Mice were fasted for 12h prior to blood collection to measure fasting glucose (ZOETIS AlphaTRAK® 2) and serum cholesterol (Molecular Probes Amplex Red Cholesterol Assay). Blood was collected by submandibular vein puncture with a sterile lancet (Braintree Scientific) followed by cervical dislocation and perfusion with 10% formalin. The brachiocephalic artery was fixed overnight in 10% formalin and processed for paraffin embedding. The heart was weighed, fixed overnight in 10% formalin and stored in 30% sucrose in PBS. Hearts were bisected horizontally at the atria and the upper portion frozen in OCT (Tissue-Tek) prior to cryosectioning. The spleen was weighed, and left tibia length measured.

Blood pressure.

Systolic and diastolic blood pressure were measured for 5 days prior to start of diet and 5 days prior to completion of treatment regime using an automated computer controlled Hatteras SC1000 (Hatteras Instruments) analysis system. The first 3 days of analysis were training and data were collected the last 2 days as previously described [19]. Each session consisted of 4 preliminary reads and 10 measurements.

Analysis of genomic recombination.

Two ApoE$^{-/-}$;N2$^{SMC\text{-}null}$ and two ApoE$^{-/-}$;N2$^{SMC\text{-}ctr}$ mice were collected one week after tamoxifen or corn oil injection. The brachiocephalic artery, brain, and aorta were collected. Brachiocephalic arteries and brain were fixed in 10% formalin before paraffin embedding.

For PCR and immunoblot, the aortic media was isolated by removing endothelium with a cotton swab and pulling a thin film of SMC away from the adventitia. Aorta and brain were flash frozen. Genomic DNA was isolated by EDTA lysis of 10mg of tissue for 3h or overnight at 55°C, precipitated with 3M sodium acetate, washed with 70% ethanol. PCR of the intact *Notch2* floxed allele with genotyping primers results in amplification of a 201bp product, while PCR of excised *Notch2* floxed does not, such that after normalizing to an internal control, the relative amplification between samples indicates excision efficiency. Intercellular adhesion molecule 1 (*ICAM1*) primers (5'-GAAATCATGTCTTGTGGAACTGA-3', 5'CTCCTTCAACAGAGAAGCCAG-3') is a control reaction with matching efficiency. Quantitative PCR was performed using Green Fast qPCR Mix LoRox (Azura) using a CFX384 thermocycler (Bio-Rad). Cycling was performed with an annealing temperature of 60°C for 40 cycles. *Notch2* C_T values were normalized to *ICAM1* C_T values and relative presence of intact *Notch2* calculated by the comparative C_T method ($2^{-\Delta\Delta C_T}$) [20].

Tissue lysates and immunoblot.

Tissues were ground in liquid nitrogen using RIPA buffer plus protease inhibitors (Sigma), sonicated, and protein quantified using the DC protein assay (Bio-Rad), mixed with Laemmli sample buffer containing 100mM dithiothreitol, and heated at 95°C for 10 minutes. SDS-PAGE was performed using TGX FastCast acrylamide 10% and 12% gels (Bio-Rad) and 15–50μg protein/lane. Gels were transferred to polyvinylidene difluoride membranes using the TransBlot Turbo Transfer System (Bio-Rad). Membranes were blocked for 10 minutes in 5% milk/PBS with 0.01% Tween-20. Primary antibodies were diluted in 5% milk and incubated overnight at 4°C: 0.2μg/mL CST 5732 rabbit anti-Notch2, 0.3μg/mL CST 3700 rabbit anti-β-actin, and 0.5μg/mL Abcam Ab53219 mouse anti-SMMHC. Membranes were incubated for 1h with HRP-linked mouse or rabbit secondary antibodies (CST) diluted in 5% milk. Signal was detected with Luminata Chemiluminescent HRP substrate (Millipore) and imaged on a ChemiDoc MP system (Bio-Rad).

Histology and immunofluorescence staining.

Brachiocephalic arteries were sectioned at 5μm from the aortic arch for ~100μm and stained with H&E. Hearts were cryosectioned through the aortic root, post fixed with 10% formalin fume, and stained with oil red O (ORO). Slides were washed in 85% propylene glycol then stained with 0.7% ORO (Sigma) in propylene glycol for 15 min at 55°C. Slides were washed in 85% propylene glycol then distilled water, counterstained with hematoxylin and coverslipped with Aquatex® aqueous mounting media (Millipore).

Formalin fixed, paraffin embedded sections were rehydrated and underwent sodium citrate antigen retrieval, 45 minutes permeabilization with 0.5% Triton X-100 (EM Scientific), blocking in PBS with 0.5% Tween-20, 2% BSA (Sigma), and 5% goat serum (Jackson ImmunoResearch) for 2h at room temperature, and with Mouse-on-Mouse Block (Vector Labs) overnight at 4°C. Sections were incubated overnight with primary antibodies in PBS/2% BSA: 1.8μg/mL rabbit anti-Notch2 (CST 4530), 1.0μg/mL rabbit anti-Notch3 (Abcam ab23426), 10μg/mL mouse anti-smooth muscle actin (SMA; Abcam ab7817), rabbit anti-IgG (CST 3900), and 10μg/mL mouse anti-IgG1 (CST 5415), 10μg/mL mouse

anti-smooth muscle actin (Abcam ab7817), 2μg/mL rat anti-Mac2 (Cedarlane CL8942AP), 10μg/mL mouse anti-IgG1 (CST 5415), and 2μg/mL rat anti-IgG2a (BioLegend 400502). Sections were washed 3× for 15 minutes in TBS-T and incubated with Alexa Fluor-conjugated secondary antibodies (Invitrogen) in 1% BSA/TBS-T for 1h at room temperature: 2μg/mL goat anti-rabbit-AF488 (A11034) and 2μg/mL goat anti-mouse-AF568 (A11077), 2μg/mL goat anti-mouse-AF488 (A11001), and 2μg/mL goat anti-rat-AF568 (A11004).

Aortic root sections were permeabilized for 5 minutes with 0.1% Tween20, then treated with 0.01mol/L sodium citrate buffer at 50°C 15 minutes. Sections were blocked in 1% BSA/TBS-T for 20 minutes before overnight incubation at 4°C with primary antibodies in 1% BSA/TBS-T: 0.12μg/mL rabbit anti-smooth muscle actin (CST 19245), 2μg/mL rat anti-Mac2 (Cedarlane CL8942AP), 0.12μg/mL rabbit anti-IgG (CST 3900), and 2μg/mL rat anti-IgG2a (BioLegend 400502). Secondary antibodies (Invitrogen) were used in 1% BSA/TBS-T for 1h at room temperature: 2μg/mL goat anti-rabbitAF488 (A11034) and 2μg/mL goat anti-rat-AF568 (A11004). Sections were washed and incubated for 2 minutes with TrueVIEW Autofluorescence Quenching Kit and coverslipped using Vectashield Hard Set anti-fade mounting medium (Vector Labs). Confocal images were captured using a Leica TCS SP8 laser scanning confocal microscope with a 10×/0.40 dry or a 63x/1.40 oil objective.

Morphometry and image analysis.

Quantification was performed while blinded to treatment group. All brachiocephalic artery sections were quantified, while for aortic roots, sections 100μm-300μm from appearance of first leaflet were used. Images were analyzed for plaque area, medial area, and necrotic core, and ORO images were also analyzed for lipid content. Images were acquired as 18μm z-stacks composed of 7 slices interspaced by 3μm, then sum slices was applied to generate 32-bit greyscale sum projections in ImageJ. Images were also analyzed for smooth muscle actin and Mac2 immunostaining. Plaque and medial areas were normalized to vessel circumference. Morphometry was performed by tracing plaques, necrotic cores, and the internal and external elastic lamina. The region of interest (ROI) manager was used to distinguish signal intensity within a specified area from total signal. For aortic roots, medial area was traced to include only areas of the vessel wall with dense elastic fiber. For ORO images, color thresholding within red hued pixels allowed for selection of ORO positive area. The smooth muscle actin and Mac2 sum projections were thresholded using the Otsu algorithm.

Statistical analysis.

The 6 week studies included 2 cohorts with 6–11 mice per cohort; the 14 week studies included 10 cohorts with 2–5 mice per cohort. Tissue sections from each mouse were utilized for each of the staining protocols. If sections from a given mouse did not survive the staining procedure, data for that stain on that mouse were not available. Statistical analysis was completed in GraphPad Prism v8.4.3, with outliers removed by ROUT testing (Q = 5%). Data are reported as mean ± SEM and compared by 2-way ANOVA and Sidak's multiple comparison test. Physiological measures were compared by 2-way ANOVA and Tukey's

multiple comparison. Differences were considered significant at $p \leq 0.05$ (*), $p \leq 0.01$ (**), $p \leq 0.001$ (***), or $p \leq 0.0001$ (****).

Results

Confirmation of SMC specific Notch2 deletion in ApoE$^{-/-}$ mice.

The use of the Notch2$^{fl/fl}$ model [15] in combination with the SMMHC-CreER^{T2} driver strain [17] resulted in reduced Notch2 protein in vascular SMC [16]. We validated this model and assessed SMC Notch2 deletion on the ApoE$^{-/-}$ background. Aorta, brachiocephalic artery, and brain were collected from 8-week-old ApoE$^{-/-}$;Notch2$^{SMC\text{-}ctr}$ and ApoE$^{-/-}$;Notch2$^{SMC\text{-}null}$ male mice one week after the last tamoxifen or corn oil injection. Smooth muscle was expected to show high efficiency of recombination and reduced Notch2 protein while neural tissue was not expected to be significantly affected by SMMHC Cre. PCR with primers flanking the upstream loxP site of the *Notch2* floxed locus results in a 201 bp band when no recombination occurs, absence of product when Cre recombination is successful, or a 161 bp wildtype band (Fig. 1A, wildtype band not present). Because amplification product results from wildtype Notch2 and non-recombined Notch2 floxed, but not from recombined Notch2 floxed, the relative amplification was used to calculate recombination efficiency. Amplification was significantly reduced for ApoE$^{-/-}$;Notch2$^{SMC\text{-}null}$ aorta derived DNA compared to all other conditions (Fig. 1B).

We also confirmed loss of vascular SMC Notch2 protein. Aorta and brain cortex from ApoE$^{-/-}$;Notch2$^{SMC\text{-}ctr}$ and ApoE$^{-/-}$;Notch2$^{SMC\text{-}null}$ mice were analyzed by immunoblot (Fig. 1C). As expected, significant SMMHC protein was detected in aorta but not brain, although Notch2 protein was present endogenously in both tissues. SMMHC expression in vascular SMC led to selective loss of Notch2 protein in the aorta from ApoE$^{-/-}$;Notch2$^{SMC\text{-}null}$ mice. Immunofluorescence staining was also performed in brain and brachiocephalic arteries from ApoE$^{-/-}$;Notch2$^{SMC\text{-}ctr}$ and ApoE$^{-/-}$;Notch2$^{SMC\text{-}null}$ mice to visualize Notch2, Notch3, and smooth muscle actin protein location within tissues (Fig. 1D). All proteins were abundantly expressed in ApoE$^{-/-}$;Notch2$^{SMC\text{-}ctr}$ brachiocephalic artery samples, while Notch2 was specifically absent in SMC in ApoE$^{-/-}$;Notch2$^{SMC\text{-}null}$ mice. Conversely, Notch2 protein was unchanged in neuronal cells of brain tissue regardless of genotype. Notch3 protein was assayed to test whether loss of SMC Notch2 would impact Notch3 levels. Notch3 protein was abundant in vessel walls for both ApoE$^{-/-}$;Notch2$^{SMC\text{-}ctr}$ and ApoE$^{-/-}$;Notch2$^{SMC\text{-}null}$ and absent in neuronal cells of brain tissue.

Physiological responses to western diet in ApoE$^{-/-}$ mice are not affected by SMC Notch2 levels.

To determine whether loss of SMC Notch2 had a systemic effect on physiological measures that can determine risk for cardiovascular disease, we measured blood pressure, weight, serum glucose and cholesterol, as well as heart weight relative to mouse size (tibia length) as an indicator of cardiac hypertrophy and spleen weight as a rough indicator of systemic inflammation [21] (Table 1). There was no difference upon loss of SMC Notch2 for any of these parameters after 6 or 14 weeks of western diet, providing support that changes in atherogenesis were due to the local cellular environment rather than systemic

changes induced by SMC Notch2 deletion. There were age-related or diet duration-related differences for systolic blood pressure, body weight post diet, fasting cholesterol, heart weight, and spleen weight.

SMC Notch2 deletion in ApoE$^{-/-}$ mice does not affect lesion size or medial area.

Cross-sectional plaque area was measured by morphometric tracing of H&E and phase contrast micrographs for brachiocephalic arteries (Fig. 2A) and ORO and phase contrast micrographs for aortic roots (Fig. 2B) then normalized to vessel circumference. Plaque area was significantly greater after 14 weeks compared to 6 weeks of western diet for both ApoE$^{-/-}$;Notch2$^{SMC\text{-}ctr}$ and ApoE$^{-/-}$;Notch2$^{SMC\text{-}null}$ mice in both regions (Fig. 2A-B, top graphs). The relative change in size of plaque between 6 and 14 weeks of western diet was greater in the brachiocephalic artery compared to the aortic root. Grouping ApoE$^{-/-}$;Notch2$^{SMC\text{-}ctr}$ and ApoE$^{-/-}$;Notch2$^{SMC\text{-}null}$ to find average plaque size for a given timepoint, plaque area was 6.5 times greater after 14 weeks compared to 6 weeks at the brachiocephalic artery while it was only 1.5 times greater at the aortic root, indicative of temporal differences in plaque accumulation in the two vessel regions. There was no significant difference in relative plaque area for ApoE$^{-/-}$;Notch2$^{SMC\text{-}ctr}$ compared to ApoE$^{/-}$;Notch2$^{SMC\text{-}null}$ mice at either timepoint in either vessel.

We observed an expansion of the media wall immediately underlying plaque compared to media with no overlying plaque. Medial expansion is a deleterious process and has been observed in acute vessel injury models [22]. Cross-sectional media area was measured to determine if medial hyperplasia was present in this disease model. We performed morphometric tracing of H&E and phase-contrast images for brachiocephalic arteries and ORO and phase-contrast images for aortic roots, and normalized areas to vessel circumference. The elastic lamina guided identification of the borders of the tunica media in the brachiocephalic arteries and aortic roots. Medial area was significantly greater after 14 weeks compared to 6 weeks of western diet for both ApoE$^{-/-}$;Notch2$^{SMC\text{-}ctr}$ and ApoE$^{-/-}$;Notch2$^{SMC\text{-}null}$ mice in brachiocephalic arteries (Fig. 2A). There was no significant difference in relative medial area for ApoE$^{-/-}$;Notch2$^{SMC\text{-}ctr}$ compared to ApoE$^{-/-}$;Notch2$^{SMC\text{-}null}$ mice at either timepoint in either vessel. The increase in medial area and circumference after 14 weeks is likely due to a combination of mouse age and plaque formation.

Atherosclerotic lesion necrosis and lipid content are independent of Notch2 in SMC.

H&E images of brachiocephalic arteries and ORO stained images of aortic roots were examined for regions of low cellularity that contained cholesterol clefts in standard pathological assessment [23]. These necrotic areas were traced and percent of total plaque area that was necrotic was calculated. Positive ORO staining within the plaque was quantified by color thresholding in ImageJ and percent of total plaque area that was lipid was calculated. There was no change in necrotic content for brachiocephalic plaques with loss of SMC Notch2, though necrosis did increase with time on western diet (Fig. 3A). There was greater necrotic content and lipid content in aortic root plaques after 6 weeks compared to 14 weeks of western diet (Fig. 3B).

SMC Notch2 deletion in ApoE$^{-/-}$ mice impacts smooth muscle actin in a time and location-dependent manner.

Cross-sectional plaque area and medial area were determined by morphometric tracing in immunofluorescence images of brachiocephalic arteries and aortic roots, then smooth muscle actin positive areas within each region were determined by image analysis (Fig. 4A & 5A). After 6 weeks of western diet, abundance of smooth muscle actin protein within brachiocephalic artery plaque was significantly reduced, and staining intensity was also significantly lower. This was quantified as % of plaque that was positive for smooth muscle actin staining and the smooth muscle actin staining intensity (total pixel grey value normalized to positive area, Fig. 4C). After 14 weeks of western diet brachiocephalic artery plaque levels of smooth muscle actin were low in both ApoE$^{-/-}$;Notch2$^{\text{SMC-ctr}}$ and ApoE$^{-/-}$;Notch$^{2\text{SMC-null}}$ mice (Fig. 4B). There was no difference in smooth muscle actin levels within aortic root plaques after 6 weeks of western diet (Fig. 5A, C) or 14 weeks (Fig. 5B, C). Percent of medial area positive for smooth muscle actin and medial layer smooth muscle actin staining intensity were significantly reduced after 14 weeks compared to 6 weeks of western diet for both genotypes at both the brachiocephalic artery and the aortic root (Fig. 4C & 5C).

SMC specific Notch2 deletion in ApoE$^{-/-}$ mice increased Mac2 staining in 6 week aortic root lesions.

Morphometric tracing of immunofluorescence images of brachiocephalic arteries and aortic roots was paired with image analysis of Mac2 positive areas (Fig. 4A & 5A). Mac2 is produced by activated macrophages [24,25] and de-differentiating SMC [11], and is used here as general measure for the presence of abnormal cells. Aortic root plaque Mac2 staining intensity was significantly higher for ApoE$^{-/-}$;Notch2$^{\text{SMC-null}}$ after 6 weeks of western diet. There was no difference in Mac2 intensity or percent plaque area between genotypes after 14 weeks at the aortic root (Fig. 5C). After 14 weeks of western diet plaque Mac2 staining intensity was significantly lower for both genotypes at both the brachiocephalic artery and the aortic root than compared to 6 weeks of western diet (Fig. 4C & 5C). Percent of plaque area Mac2 positive was significantly lower at 14 weeks of western diet compared to 6 weeks in both genotypes at the brachiocephalic artery (Fig. 4C) but not at the aortic root (Fig. 5C).

Discussion/Conclusion

Temporal analysis of lesion progression.

Comparison of lesions between the 6 week and 14 week timepoints revealed that several factors changed predictably with time for both athero-prone vascular regions. As expected with untreated hypercholesteremia, plaques were larger after 14 weeks of western diet than they were after 6 weeks. Also as expected, plaques at the brachiocephalic artery were more necrotic after 14 weeks of western diet than they were after 6 weeks. However, there was a surprising decrease in necrotic plaque area and lipid content after 14 weeks at the aortic root. Atherosclerosis is not a simple process of greater and greater necrosis and greater and greater lipid accumulation, but rather a complex series of responses from a myriad of vascular cells that cause changes to matrix, cell growth, and remodeling. Indeed, the opposing direction of change in necrotic content between 6 and 14 weeks

of western diet at the aortic root compared to the brachiocephalic artery indicate that not only is atherosclerosis a complex process, but it is also complex in how it impacts specific sites at given timepoints. Remodeling of extracellular matrix and the migration of cells throughout the plaque may contribute to these changes. Interestingly, Mac2 positive area and/or intensity was decreased after 14 weeks. Mac2 is commonly used as an inflammatory marker and because advanced lesions are typically characterized by robust inflammation, this observation was not expected. However, it was recently found that Mac2 positive macrophages were replaced with Mac2 negative macrophages over time and that unstable plaques were more likely to contain greater numbers of Mac2 negative macrophages [26]. Loss of macrophage Mac2 was hypothesized to promote an invasive proinflammatory phenotype that destabilized plaque. It was also recently observed that not only did populations of lesion SMC activate Mac2 expression [8,27], but that subpopulations then went on to lose Mac2 expression [11]. It is unknown whether loss of Mac2 expression in lesion SMC stabilizes or destabilizes plaque. Another factor that changed consistently over time at both vessel locations was reduction of contractile marker smooth muscle actin in the medial layer. This was consistent with the finding that smooth muscle actin in the tunica media of the aortic root was reduced in advanced atherosclerosis [28]. This loss of contractile protein in the media may have been a harbinger of increased SMC motility into lesions and reduced vascular contractility. A related finding in brachiocephalic arteries was increased cross-sectional area, or medial thickening, over time. Medial thickening could be caused by SMC transition to a proliferative phenotype.

SMC Notch2 in SMC in contractile phenotype.

Deletion of SMC Notch2 resulted in lower contractile smooth muscle actin protein level in the brachiocephalic artery after 6 weeks of western diet. No significant changes to smooth muscle actin content were observed within lesions or media at the aortic root after 6 weeks of western diet or in either vessel bed after 14 weeks. Previously we found that human SMC derived from endarterectomy samples were unable to upregulate smooth muscle actin upon treatment with Jagged1 indicating loss of Notch mediated maintenance of differentiation for SMC in late atherosclerosis [13]. In this in vivo study, reduced smooth muscle actin in brachiocephalic artery lesions upon loss of Notch2 signaling in vascular SMC points to functional Notch mediated maintenance of SMC differentiation early in atherosclerosis. Reduced expression of contractile proteins in lesion SMC has been shown to be deleterious in two major ways. SMC in lesions with the contractile phenotype are typically found near the lumenal face and contribute to the lumenal fibrous cap; loss of this protective layer predisposes lesions to rupture [29]. Additionally, permanent or transitory transition of lesion SMC from a contractile phenotype to a macrophage-like phenotype leads to formation of foam cells and cholesterol accumulation [30,31]. Our results from mice fed western diet for 14 weeks reveal that Notch2 signaling does not impact late atherosclerosis, though it may have a minor role in plaque stabilization early in atherosclerosis. One potential limitation of our study is the possible re-emergence of newly differentiated SMC after the tamoxifeninduction period. Because mature SMC are predicted to contribute to the majority of foam cells within atherosclerotic plaques in humans and mice [32], we believe that targeting of mature SMC prior to atheroma formation is a likely strategy to target Notch2 in SMC-derived populations in the plaque.

Recently it has been shown that cells other than SMC may express smooth muscle actin within the plaque environment thus contributing to lesion stability[33]. Newman et al. generated SMC-PDGFRβ null mice with simultaneous SMC lineage tracing on an ApoE$^{-/-}$ background and observed endothelial cells and macrophages that had transitioned to mesenchymal-like cells that expressed smooth muscle actin and contributed to plaque stability. Loss of SMC-PDGFRβ resulted in 90% less investment of SMC into lesions, yet the plaques did not differ in size, stability, or number of smooth muscle actin positive cells compared to littermate controls. They provide evidence that mesenchymal-like cells compensated for reduced SMC in atherosclerotic plaques, at least temporarily. In the current study we saw instances when loss of SMC-Notch2 resulted in changes to lesion smooth muscle actin or Mac2 content, yet lesion size never changed. It is possible that Notch2 null SMC in our model had reduced function that was compensated for by non-SMC cell types. Without lineage tracing, our study provided insight into total smooth muscle actin in lesions. Because the Newman et al study showed that SMC derived smooth muscle actin contribution to plaque stability can be temporarily compensated for by endothelial cell and macrophage derived mesenchymal cells, future studies of notch signaling in atherosclerotic lesions should include linage tracing. Lesions likely to lose stability due to loss of SMC specific smooth muscle actin cannot be detected without additional interrogation of cellular origin.

Vessel beds have distinct response to loss of SMC Notch2.

SMC of the aortic root derive from the secondary heart field of lateral plate mesoderm, while brachiocephalic artery SMC come from neural crest [34]. There is evidence that differences in SMC origin influence the function of the mature vessel and the constituent SMC [35,36]. If the role of Notch2 in regulating SMC phenotype varies between SMC of different developmental origins, this might explain why SMC Notch2 maintains lesion SMC in a contractile phenotype at the brachiocephalic artery yet prevents transition to and/or accumulation of Mac2 positive cells at the aortic root after 6 weeks of western diet. Alternatively, because a 6 week brachiocephalic lesion is likely to be developmentally younger than a 6 week aortic root lesion [37], these differences in vessel bed response to loss of SMC Notch2 could be a reflection of different roles for SMC Notch2 through disease progress. Overall, our study indicates a minor role for Notch2 in regulating SMC in atherogenesis in a location and temporally dependent manner.

Acknowledgement

The authors acknowledge the expert assistance of the Histopathology Core Facility at Maine Medical Center Research Institute (Dr. V. Lindner and G. Mangoba) and our Confocal Microscopy Facility (Dr. I. Prudovsky).

Funding Sources

This study was supported by NIH/NHLBI grant R01 HL141149 to LL. JDK was supported by a predoctoral fellowship from the American Heart Association (16PRE29870001). Our institutional Histopathology Core facility is supported by NIH/NIGMS award 1P20GM12130 to LL and NIH/NIGMS award U54GM115516 (C. Rosen and G. Stein, PIs).

Literature Cited

1. Briot A, Civelek M, Seki A, Hoi K, Mack JJ, Lee SD, et al. Endothelial NOTCH1 is suppressed by circulating lipids and antagonizes inflammation during atherosclerosis. J Exp Med. 2015;212(12):2147–63. [PubMed: 26552708]
2. Mack JJ, Mosqueiro TS, Archer BJ, Jones WM, Sunshine H, Faas GC, et al. NOTCH1 is a mechanosensor in adult arteries. Nat Commun. 2017;8(1):1620. [PubMed: 29158473]
3. Fung E, Tang S-MT, Canner JP, Morishige K, Arboleda-Velasquez JF, Cardoso AA, et al. Delta-Like 4 Induces Notch Signaling in Macrophages. Circulation. 2007 Jun;115(23):2948–56. [PubMed: 17533181]
4. Monsalve E, Ruiz-García A, Baladrón V, Ruiz-Hidalgo MJ, Sánchez-Solana B, Rivero S, et al. Notch1 upregulates LPS-induced macrophage activation by increasing NFκB activity. Eur J Immunol. 2009 Sep;39(9):2556–70. [PubMed: 19662631]
5. Fukuda D, Aikawa E, Swirski FK, Novobrantseva TI, Kotelianski V, Gorgun CZ, et al. Notch ligand delta-like 4 blockade attenuates atherosclerosis and metabolic disorders. Proc Natl Acad Sci U S A. 2012;109(27):E1868–77.
6. Boucher J, Gridley T, Liaw L. Molecular pathways of notch signaling in vascular smooth muscle cells. Front Physiol. 2012;3 APR(April):1–13. [PubMed: 22275902]
7. Baeten JT, Lilly B. Notch Signaling in Vascular Smooth Muscle Cells. Adv Pharmacol. 2017;78:351–82. [PubMed: 28212801]
8. Shankman LS, Gomez D, Cherepanova OA, Salmon M, Alencar GF, Haskins RM, et al. KLF4 Dependent Phenotypic Modulation of SMCs Plays a Key Role in Atherosclerotic Plaque Pathogenesis Laura. Nat Med. 2015;21(6):628–37. [PubMed: 25985364]
9. Albarrán-Juárez J, Kaur H, Grimm M, Offermanns S, Wettschureck N. Lineage tracing of cells involved in atherosclerosis. Atherosclerosis. 2016;251:445–53. [PubMed: 27320174]
10. Jacobsen K, Lund MB, Shim J, Gunnersen S, Füchtbauer E-M, Kjolby M, et al. Diverse cellular architecture of atherosclerotic plaque derives from clonal expansion of a few medial SMCs. JCI Insight. 2017 Oct;2(19):1–13.
11. Alencar GF, Owsiany KM, Karnewar S, Sukhavasi K, Mocci G, Nguyen AT, et al. Stem Cell Pluripotency Genes Klf4 and Oct4 Regulate Complex SMC Phenotypic Changes Critical in Late-Stage Atherosclerotic Lesion Pathogenesis. Circulation. 2020 Nov;2045–59.
12. Boucher JM, Harrington A, Rostama B, Lindner V, Liaw L. A receptor-specific function for Notch2 in mediating vascular smooth muscle cell growth arrest through cyclin-dependent kinase inhibitor 1B. Circ Res. 2013;113(8):975–85. [PubMed: 23965337]
13. Davis-knowlton J, Turner JEJEJE, Turner A, Damian-Loring S, Hagler N, Henderson T, et al. Characterization of smooth muscle cells from human atherosclerotic lesions and their responses to Notch signaling. Lab Investig. 2018 Mar;99(3):290–304. [PubMed: 29795127]
14. Martos-Rodríguez CJ, Albarrán-Juárez J, Morales-Cano D, Caballero A, Macgrogan D, De La Pompa JL, et al. Fibrous Caps in Atherosclerosis Form by Notch-Dependent Mechanisms Common to Arterial Media Development. Arterioscler Thromb Vasc Biol. 2021;E427–39. [PubMed: 34261328]
15. McCright B, Lozier J, Gridley T. Generation of new Notch2 mutant alleles. Genesis. 2006;44(1):29–33. [PubMed: 16397869]
16. Peterson SM, Turner JE, Harrington A, Davis-Knowlton J, Lindner V, Gridley T, et al. Notch2 and proteomic signatures in mouse neointimal lesion formation. Arterioscler Thromb Vasc Biol. 2018 Jul;38(7):1576–93. [PubMed: 29853569]
17. Wirth A, Benyó Z, Lukasova M, Leutgeb B, Wettschureck N, Gorbey S, et al. G12G13-LARG-mediated signaling in vascular smooth muscle is required for salt-induced hypertension. Nat Med. 2008;14(1):64–8. [PubMed: 18084302]
18. Piedrahita JA, Zhang SH, Hagaman JR, Oliver PM, Maeda N. Generation of mice carrying a mutant apolipoprotein E gene inactivated by gene targeting in embryonic stem cells. Proc Natl Acad Sci U S A. 1992;89(10):4471–5. [PubMed: 1584779]

19. Jaffe IZ, Newfell BG, Aronovitz M, Mohammad NN, McGraw AP, Perreault RE, et al. Placental growth factor mediates aldosterone-dependent vascular injury in mice. J Clin Invest. 2010 Nov;120(11):3891. [PubMed: 20921624]
20. Schmittgen TD, Livak KJ. Analyzing real-time PCR data by the comparative C(T) method. Nat Protoc. 2008 [cited 2019 Mar 29]. ;3(6):1101–8. [PubMed: 18546601]
21. Buchan L, St Aubin CR, Fisher AL, Hellings A, Castro M, Al-Nakkash L, et al. Highfat, high-sugar diet induces splenomegaly that is ameliorated with exercise and genistein treatment. BMC Res Notes. 2018 Oct;11(1):752. [PubMed: 30348225]
22. Kumar A, Lindner V. Remodeling With Neointima Formation in the Mouse Carotid Artery After Cessation of Blood Flow. Arterioscler Thromb Vasc Biol. 1997 Oct;17(10):2238–44. [PubMed: 9351395]
23. Seimon TA, Wang Y, Han S, Senokuchi T, Schrijvers DM, Kuriakose G, et al. Macrophage deficiency of p38α MAPK promotes apoptosis and plaque necrosis in advanced atherosclerotic lesions in mice. J Clin Invest. 2009 Apr;119(4):886. [PubMed: 19287091]
24. Sato S, Hughes RC. Regulation of secretion and surface expression of Mac-2, a galactoside-binding protein of macrophages. J Biol Chem. 1994 Feb;269(6):4424–30. [PubMed: 8308013]
25. Liu FT, Hsu DK, Zuberi RI, Kuwabara I, Chi EY, Henderson WR. Expression and function of galectin-3, a β-galactoside-binding lectin, in human monocytes and macrophages. Am J Pathol. 1995 [cited 2021 Feb 27]. ;147(4):1016–28. [PubMed: 7573347]
26. Di Gregoli K, Somerville M, Bianco R, Thomas AC, Frankow A, Newby AC, et al. Galectin-3 Identifies a Subset of Macrophages with a Potential Beneficial Role in Atherosclerosis. Arterioscler Thromb Vasc Biol. 2020;40:1491–509. [PubMed: 32295421]
27. Feil S, Fehrenbacher B, Lukowski R, Essmann F, Schulze-Osthoff K, Schaller M, et al. Transdifferentiation of vascular smooth muscle cells to macrophage-like cells during atherogenesis. Circ Res. 2014 Sep;115(7):662–7. [PubMed: 25070003]
28. Moss ME, DuPont JJ, Iyer SL, McGraw AP, Jaffe IZ. No Significant Role for Smooth Muscle Cell Mineralocorticoid Receptors in Atherosclerosis in the ApolipoproteinE Knockout Mouse Model. Front Cardiovasc Med. 2018;5:81. [PubMed: 30038907]
29. Hansson GK, Libby P, Tabas I. Inflammation and plaque vulnerability. J Intern Med. 2015;278(5). DOI: 10.1111/joim.12406
30. Allahverdian S, Chehroudi AC, McManus BM, Abraham T, Francis GA. Contribution of intimal smooth muscle cells to cholesterol accumulation and macrophage-like cells in human atherosclerosis. Circulation. 2014;129(15). DOI: 10.1161/CIRCULATIONAHA.113.005015
31. Li Y, Zhu H, Zhang Q, Han X, Zhang Z, Shen L, et al. Smooth muscle-derived macrophage-like cells contribute to multiple cell lineages in the atherosclerotic plaque. Cell Discov 2021 71. 2021 Nov;7(1):1–4. [PubMed: 33390590]
32. Wang Y, Dubland JA, Allahverdian S, Asonye E, Sahin B, Jaw JE, et al. Smooth Muscle Cells Contribute the Majority of Foam Cells in ApoE (Apolipoprotein E)-Deficient Mouse Atherosclerosis. Arterioscler Thromb Vasc Biol. 2019 May;39(5):876–87. [PubMed: 30786740]
33. Newman AAC, Serbulea V, Baylis RA, Shankman LS, Bradley X, Alencar GF, et al. Multiple cell types contribute to the atherosclerotic lesion fibrous cap by PDGFRβ and bioenergetic mechanisms. Nat Metab. 2021;3(2):166–81. [PubMed: 33619382]
34. Sinha S, Iyer D, Granata A. Embryonic origins of human vascular smooth muscle cells: implications for in vitro modeling and clinical application. Cell Mol Life Sci. 2014 Jun;71(12):2271–88. [PubMed: 24442477]
35. Zhang J, Chen J, Xu C, Yang J, Guo Q, Hu Q, et al. Resveratrol inhibits phenotypic switching of neointimal vascular smooth muscle cells after balloon injury through blockade of Notch pathway. J Cardiovasc Pharmacol. 2014;63(3):233–9. [PubMed: 24603118]
36. Jiao J, Xiong W, Wang L, Yang J, Qiu P, Hirai H, et al. Differentiation defect in neural crest-derived smooth muscle cells in patients with aortopathy associated with bicuspid aortic valves. EBioMedicine. 2016;10:282. [PubMed: 27394642]
37. Nakashima Y, Plump AS, Raines EW, Breslow JL, Ross R. ApoE-deficient mice develop lesions of all phases of atherosclerosis throughout the arterial tree. Arterioscler Thromb A J Vasc Biol. 1994;14(1):133–40.

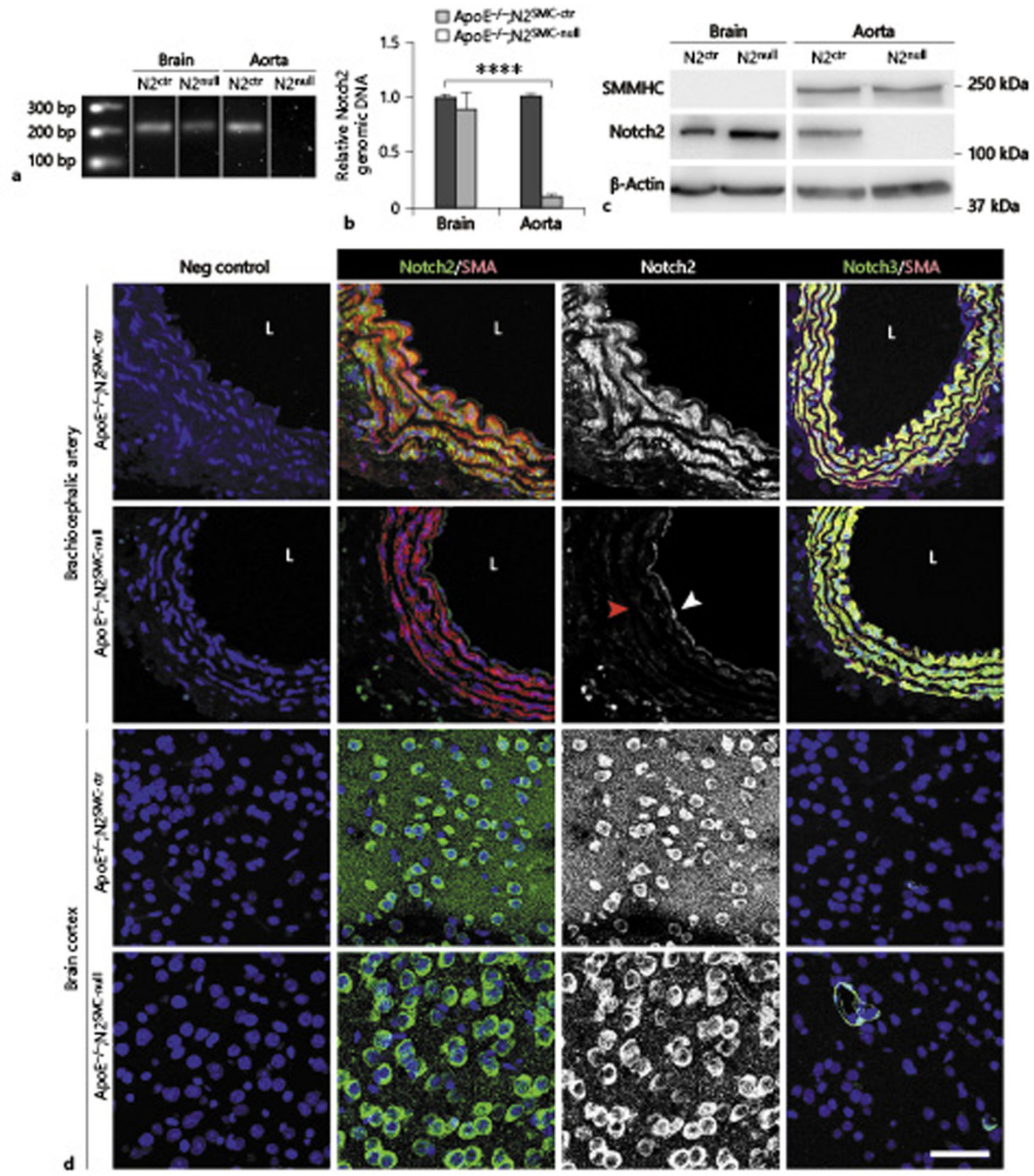

Fig. 1. Notch2 deletion in vascular SMC in ApoE−/− mice.

A) Genomic DNA was collected one week after Cre induction from brain cortex and aorta for PCR amplification. Shown are representative PCR products from ApoE$^{-/-}$;Notch2$^{SMC\text{-}ctr}$ (N2^{ctr}) and ApoE$^{-/-}$;Notch2$^{SMC\text{-}null}$ (N2^{null}) mice. The *Notch2* floxed allele generates a 201bp fragment, which was specifically lost from the aorta in N2^{null} mice, indicating Cre recombination. B) PCR amplification data were quantified, and technical replicates were compared in two-way ANOVA. Significant results of Dunnett's multiple comparisons test of each condition to ApoE$^{-/-}$;Notch2$^{SMC\text{-}ctr}$ brain are indicated by asterisks. Amplification

from the $N2^{null}$ aorta was significantly lower, ****$p \leq 0.0001$ compared to the other three groups. C) Representative immunoblot for SMMHC and Notch2 with brain cortex and aorta lysates from $ApoE^{-/-}$;$Notch2^{SMC\text{-}ctr}$ ($N2^{ctr}$) and $ApoE^{-/-}$;$Notch2^{SMC\text{-}null}$ ($N2^{null}$) mice, with b-actin as a loading control. Molecular weights indicate molecular weight markers. D) Brachiocephalic artery and brain cortex sections were immunostained for Notch2/smooth muscle actin (SMA) or Notch3/SMA with DAPI nuclear staining. Nonimmune IgG and IgG1 stained sections are shown as negative controls. L=lumen. Endothelial cells (white arrow) retain Notch2 protein in arteries. Red arrowhead highlights Notch2 negative SMC next to Notch2 positive endothelial cells (white arrowhead). Scale bar=50μm.

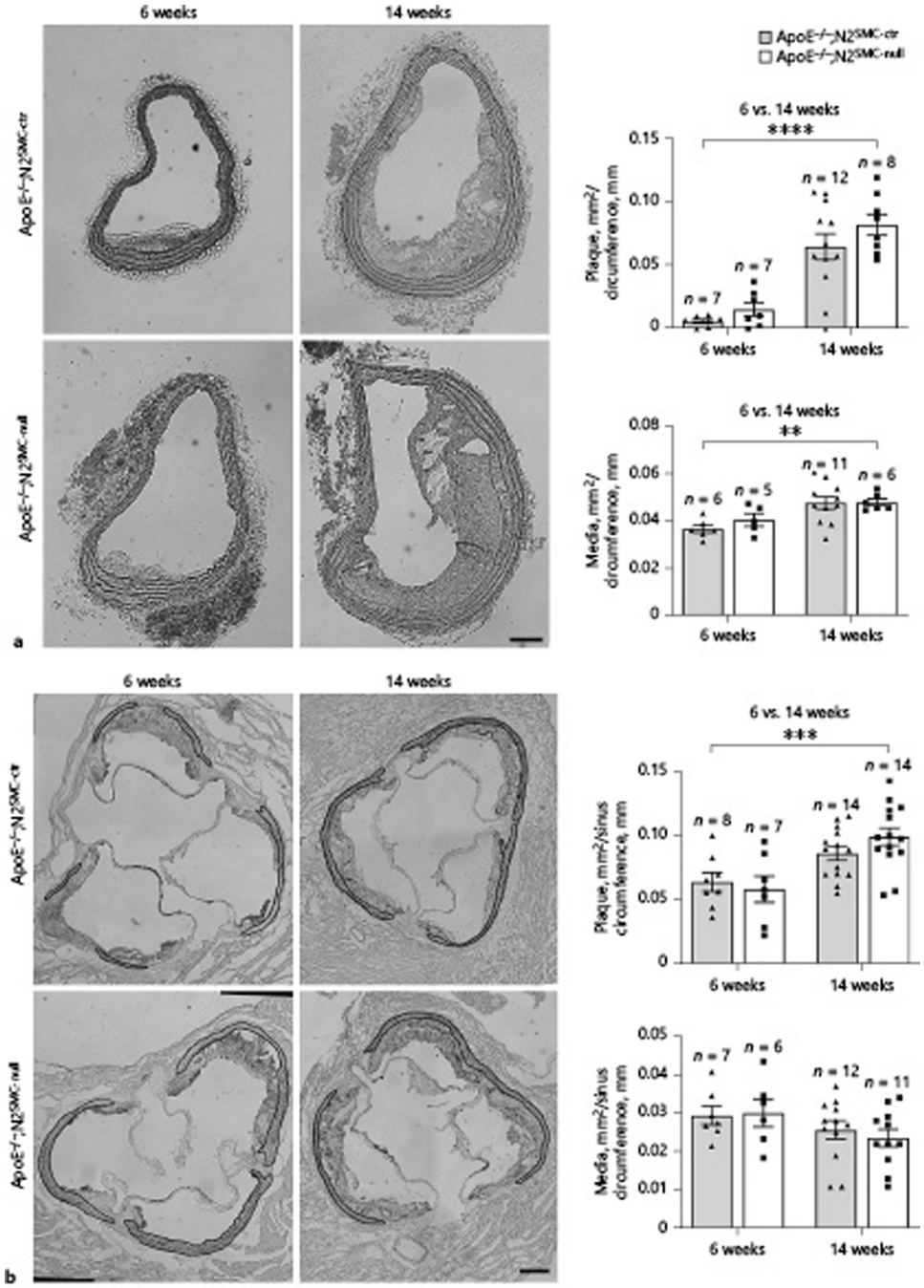

Fig. 2. Overall plaque size does not change with loss of SMC Notch2.

Mice with the genotypes indicated were fed a western diet for 6 or 14 weeks. A) Representative brachiocephalic artery images with morphometric quantification of relative plaque size and medial area in ApoE$^{-/-}$;Notch2$^{SMC\text{-}ctr}$ and ApoE$^{-/-}$;Notch2$^{SMC\text{-}null}$ mice. Scale bar = 100μm. No significant results were found by Sidak's multiple comparisons test (genotype). Significant differences between 6 week and 14 weeks of diet found using 2way ANOVA are indicated by asterisks: **p ≤ 0.01, ****p ≤ 0.0001. B) Representative aortic root images with morphometric quantification of relative plaque size and medial

area in ApoE$^{-/-}$;Notch2$^{SMC\text{-}ctr}$ and ApoE$^{-/-}$;Notch2$^{SMC\text{-}null}$ mice after 6 or 14 weeks of western diet. The thin solid black lines demarcate the medial layer. Scale bar = 200μm. No significant results were found by Sidak's multiple comparisons test based on genotype. Significant differences between 6 week and 14 weeks of diet found using 2way ANOVA are indicated by asterisks: ***$p \leq 0.001$. Although there were no differences by genotype, plaque circumference was significantly higher (***$p \leq 0.001$) comparing all mice fed western diet for 14 weeks to all mice on western diet for 6 weeks by 2-way ANOVA.

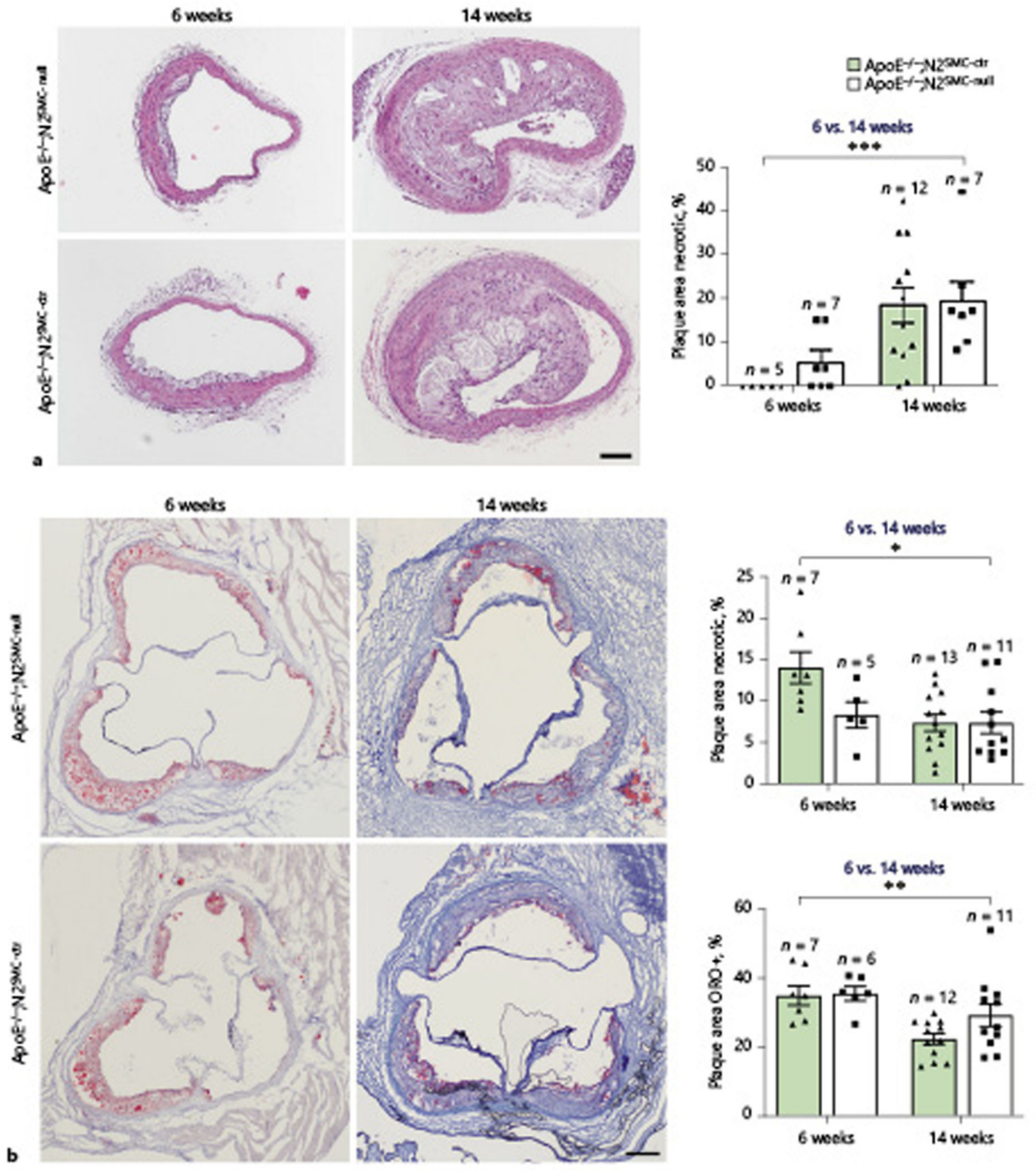

Fig. 3. Cellularity and lipid content in the plaque are not affected by loss of Notch2 in SMC.

Mice with the genotypes indicated were fed a western diet for 6 or 14 weeks. A) Representative brachiocephalic artery histological images with morphometric quantification of lesion necrosis in ApoE$^{-/-}$;Notch2$^{SMC\text{-}ctr}$ and ApoE$^{-/-}$;Notch2$^{SMC\text{-}null}$ mice after 6 or 14 weeks. Scale bar = 100μm. No significant results were found by Sidak's multiple comparisons test based on genotype. Significant differences between 6 week and 14 weeks of diet were found using 2-way ANOVA, ***$p \leq 0.001$. B) Representative aortic root sections stained with oil red O. Scale bar = 200μm. Non-cellular areas and lipid containing

areas were quantified No significant results were found by Sidak's multiple comparisons test comparing genotype. Significant differences between 6 week and 14 weeks of diet found using 2-way ANOVA are indicated by asterisks: *$p \leq 0.05$, **$p \leq 0.01$.

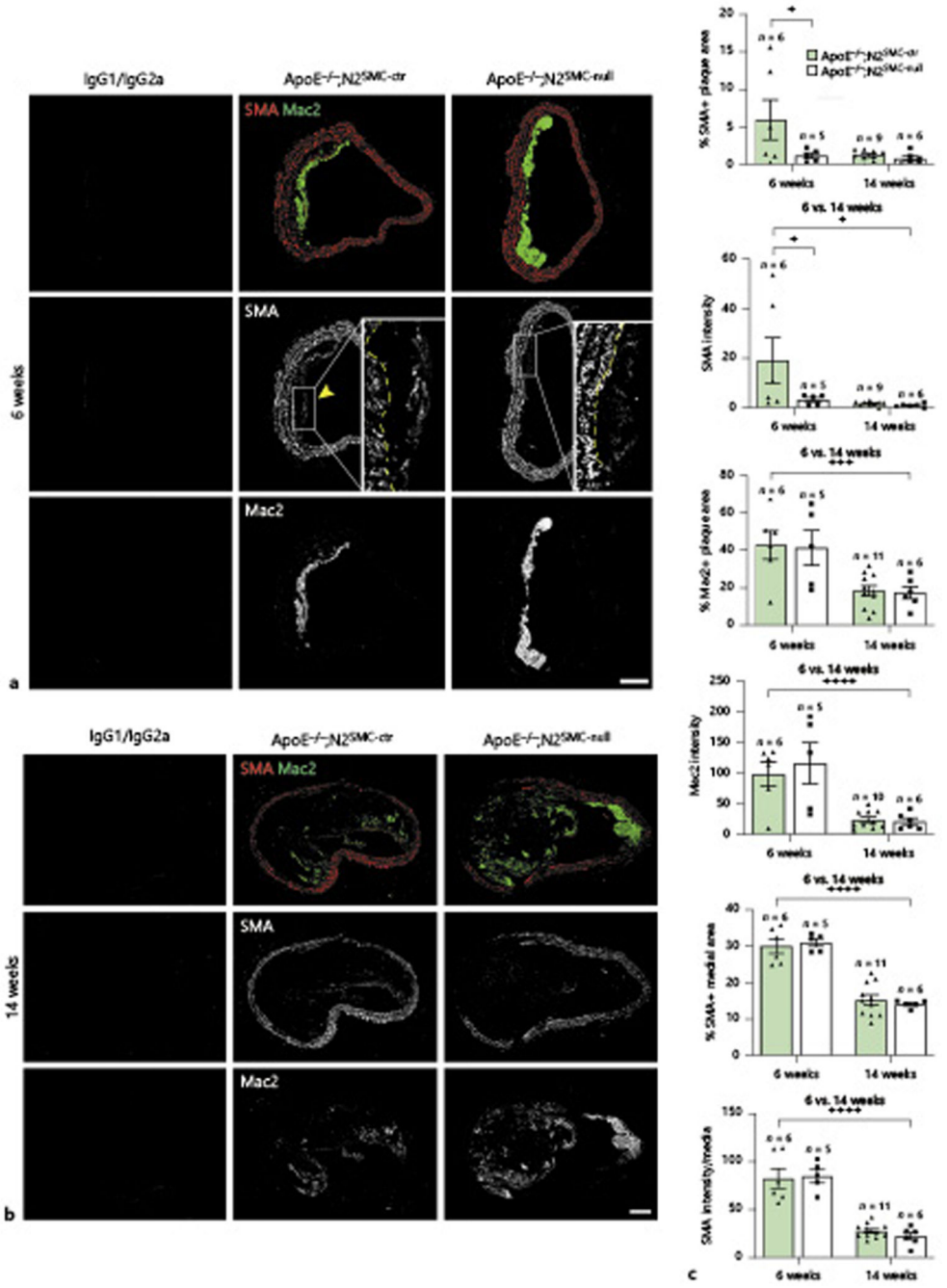

Fig. 4. Smooth muscle actin is reduced in early brachiocephalic artery plaque with loss of Notch2 in SMC.

Mice with the genotypes indicated were fed a western diet for 6 (A) or 14 (B) weeks. Representative immunofluorescent images of brachiocephalic artery lesions from ApoE$^{-/-}$;Notch2$^{SMC\text{-}ctr}$ and ApoE$^{-/-}$;Notch2$^{SMC\text{-}null}$ mice. Smooth muscle actin (SMA) is labeled in red, and Mac2 is labeled in green, and each is also shown individually to better show plaque SMA (yellow arrowheads in panel A). Scale bars = 100μm. C) Morphometric quantification of plaque SMA content, plaque Mac2 content, and medial SMA content in ApoE$^{-/-}$;Notch2$^{SMC\text{-}ctr}$ and ApoE$^{-/-}$;Notch2$^{SMC\text{-}null}$ mice after 6 or 14

weeks of western diet. Sidak's multiple comparisons test showed that % SMA+ plaque area was significantly decreased at 6 weeks in the $ApoE^{-/-}$;$Notch2^{SMC\text{-}null}$ mouse, *p ≤ 0.05. Significant differences were found between 6 week and 14 weeks of diet for all the other measures using 2-way ANOVA: *p ≤ 0.05, ***p ≤ 0.001, ****p ≤ 0.0001.

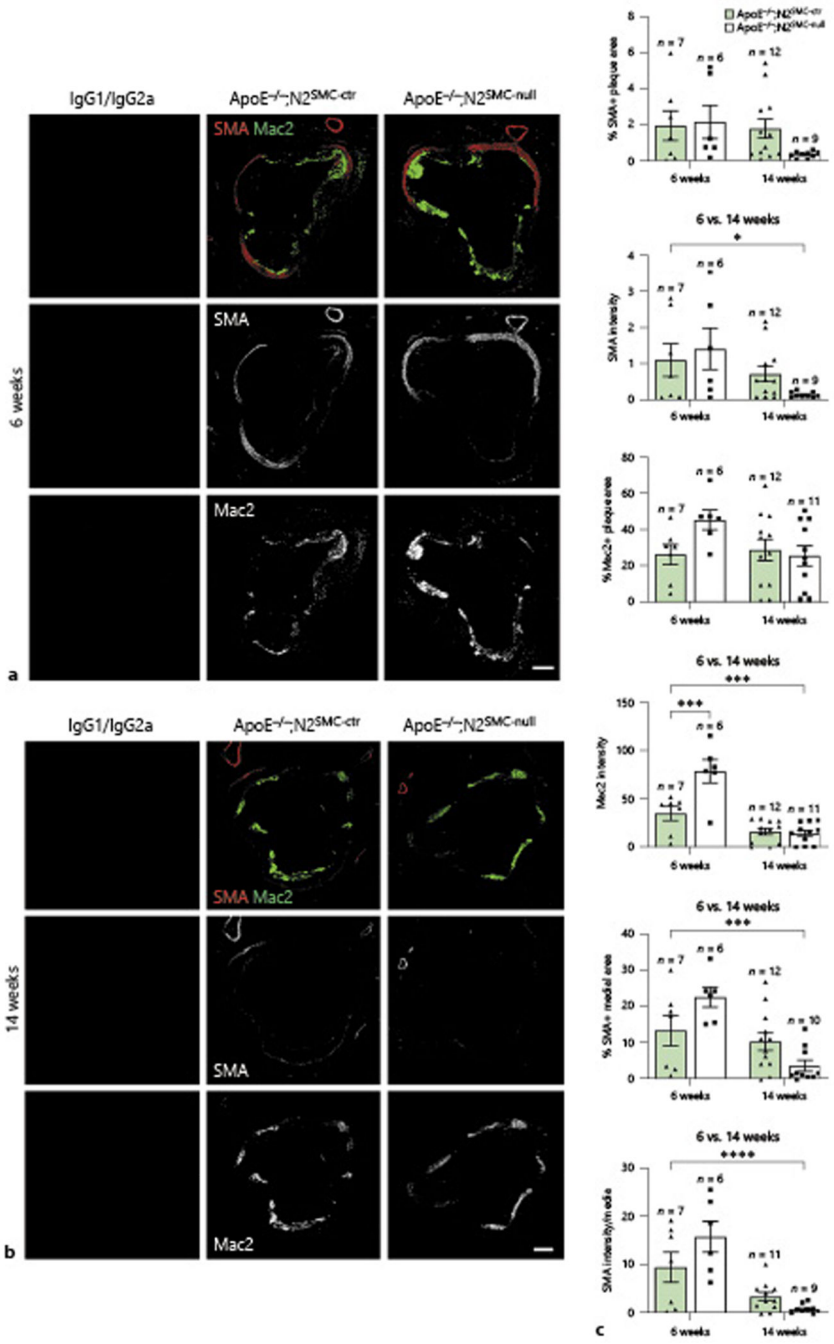

Fig. 5. Aortic root plaque Mac2 is increased with loss of SMC Notch2.

Representative immunofluorescent images of aortic root lesions from ApoE$^{-/-}$;Notch2$^{SMC\text{-}ctr}$ and ApoE$^{-/-}$;Notch2$^{SMC\text{-}null}$ mice after 6 weeks (A) or 14 weeks (B) of western diet. Smooth muscle actin (SMA) is in red, and Mac2 is in green. Individual staining patterns are also shown. Scale bars = 200μm. C) Morphometric quantification of plaque SMA content, plaque Mac2 content, and media SMA content in ApoE$^{-/-}$;Notch2$^{SMC\text{-}ctr}$ and ApoE$^{-/-}$;Notch2$^{SMC\text{-}null}$ mice after 6 or 14 weeks of western diet. Sidak's multiple comparisons test was used to compare groups by genotype – the

only statistically significant differences was the Mac2 intensity at 6 weeks, ***$p \leq 0.001$. Significant differences between 6 week and 14 weeks of diet found using 2-way ANOVA are indicated by asterisks: *$p \leq 0.05$, ***$p \leq 0.001$, ****$p \leq 0.0001$.

Table 1.

Physiological measurements in ApoE$^{-/-}$;Notch2$^{SMC\text{-}ctr}$ and ApoE$^{-/-}$;Notch2$^{SMC\text{-}null}$ mice after 6 and 14 weeks of western diet.

Time on Western diet	**6 weeks**		**14 weeks**	
Genotype	**ApoE$^{-/-}$; Notch2$^{SMC\text{-}ctr}$**	**ApoE$^{-/-}$; Notch2$^{SMC\text{-}null}$**	**ApoE$^{-/-}$; Notch2$^{SMC\text{-}ctr}$**	**ApoE$^{-/-}$; Notch2$^{SMC\text{-}null}$**
Systolic BP‡, mmHg	126 ± 7.3 (5)	117 ± 4.7 (6)	140 ± 4.4 (16)	134 ± 4.7 (17)
Diastolic BP, mmHg	72 ± 13.4 (5)	74 ± 8.7 (6)	90 ± 4.5 (16)	85 ± 3.8 (15)
Weight post-diet‡, g	26.5 ± .07 (8)	26.7 ± 0.6 (9)	34 ± 1.4 (16)$^{\#}$	34 ± 1.1 (17)$^{\#}$
Fasting glucose, mg/dL	130 ± 3.6 (8)	129 ± 6.3 (9)	151 ± 9.6 (17)	137 ± 6.7 (17)
Fasting cholesterol‡, mg/dL	528 ± 19.1 (7)	606 ± 21.0 (9)	761 ± 58.0 (17)	697 ± 40.9 (17)
Heart weight‡, mg/mm tibia length	11.81 ± 0.68 (8)	10.5 ± 0.5 (8)	16 ± 1.09 (13)$^{\#}$	13.2 ± 0.62 (15)$^{\#}$
Spleen weight‡, mg	165 ± 6.3 (8)	159 ± 13.2 (9)	368 ± 23.1 (15)$^{\#}$	393 ± 36.2 (17)$^{\#}$

Data are presented as mean ± SEM, with *N* shown in parentheses for each measurement. BP, blood pressure; SMC, smooth muscle cell.

‡Significant differerce between 6- and 14-week Western diet by ANOVA.

$^{\#}$ $p \leq 0.05$ versus genotype-matched 6-week Western diet (Tukey test).